RSC Advances

PAPER

Cite this: *RSC Adv.*, 2020, **10**, 8917

Formulation and polymerization of foamed 1,4-BDDMA-in-water emulsions†

Miriam Lucia Dabrowski,[a] Martin Hamann[ab] and Cosima Stubenrauch *[a]

Received 9th January 2020
Accepted 20th February 2020

DOI: 10.1039/d0ra00254b

rsc.li/rsc-advances

Emulsion and foam templating allow the synthesis of tailor-made polymer foams. A complementary templating route is foamed emulsion templating. The concept is based on the generation of a monomer-in-water emulsion which is subsequently foamed. After polymerization of the foamed emulsion, one obtains open-cell polymer foams with porous pore walls. In the paper at hand, we generated foamed emulsions and synthesized polymer foams which are based on the monomer 1,4-butanediol dimethacrylate (1,4-BDDMA). The main challenge was to find the optimal composition of the emulsion by varying the components systematically. We will discuss that the composition of the monomer-in-water emulsion is key for the stability of the foamed emulsion and thus for the structure of the resulting polymer foam. The final composition of the continuous phase was found to be 65 vol% 1,4-BDDMA, 30 vol% water and 5 vol% glycerol. We foamed and polymerized this emulsion to check the foamed emulsion's suitability as a template for solid polymer foams. We generated a foamed emulsion with a mean bubble diameter of 151 μm ± 90 μm and obtained a highly porous poly(1,4-BDDMA) foam with a pore mean diameter of 366 μm ± 91 μm. Furthermore, the polymer foam has a "sub-porosity" within the pore walls.

1. Introduction

The synthesis of tailor-made polymer foams gains increasing attention focusing on polymer foams with specific properties for different applications. One of these applications is tissue engineering in which polymer foams are used as scaffolds for the seeding and growing of cells.[1] For tissue engineering purposes, polymer foams have to meet the following requirements. The scaffold itself has to be highly porous with interconnected pores around 50 μm to 500 μm and the material of the matrix has to be biodegradable, biocompatible and cytocompatible.[1–5] A large number of studies tackle the synthesis and characterization of polymer foams for tissue engineering *via* liquid templating routes, namely emulsion templating and foam templating. Emulsion templating is usually carried out with water-in-oil or oil-in-water emulsion. In the first case, the hydrophobic continuous phase consists of monomers such as propylene fumarate[6] and propylene fumarate dimethacrylate (PFDMA).[7,8] In the second case, the hydrophilic continuous phase usually consists of polymers such as alginates,[9] modified gelatin,[10–12] chitosan,[13,14] furfuryl alcohol[15] or dextran-methacrylate.[10,16] For foam templating, on the other hand, liquid foams are used as structuring templates for the synthesis of solid foams. Typically, aqueous solutions of (bio-) polymers such as chitosan[17–22] or (modified) gelatin[23–28] that contain a surfactant and a crosslinking agent are used for this templating route. In the first step, the aqueous solution is foamed *via* bubbling, stirring, or microfluidics. After foaming, the crosslinking reaction sets in and solidifies the foam's continuous phase. As a result, a solid polymer foam with the porous structure of the initial liquid foam is obtained.

Salonen *et al.* and Schüler *et al.* created the novel concept of foamed emulsion templating combining emulsion and foam templating.[29,30] The former study deals with the fundamental physics of foamed oil-in-water emulsions by using non-polymerizable oils, whereas the latter study focuses on the synthesis of polymer foams using styrene as monomer. The overall concept was described in detail in ref. 30 and will be briefly explained in the following (Scheme 1). (1) The first step is the preparation of a monomer-in-water emulsion, which is the continuous phase of the foamed emulsion. Here, the emulsion consisted of styrene, water, the surfactant sodium dodecylsulfate (SDS), and glycerol. The emulsion is ultrasonically homogenized and (2) foamed with a KPG stirrer equipped with a commercial milk frother. Note that the surfactant is used to stabilize both the monomer-in-water emulsion and the foamed emulsion. The next steps are the polymerization (3) and purification (4) of the polymer foam. Following this concept, foamed styrene-in-water emulsions with a mean

[a]*Institute of Physical Chemistry, University of Stuttgart, Pfaffenwaldring 55, 70569 Stuttgart, Germany. E-mail: cosima.stubenrauch@ipc.uni-stuttgart.de; Tel: +49-711-685 64470*

[b]*Institut Charles Sadron, CNRS UPR22, Université de Strasbourg, 23 Rue Du Loess, 67200 Strasbourg, France*

† Electronic supplementary information (ESI) available. See DOI: 10.1039/d0ra00254b

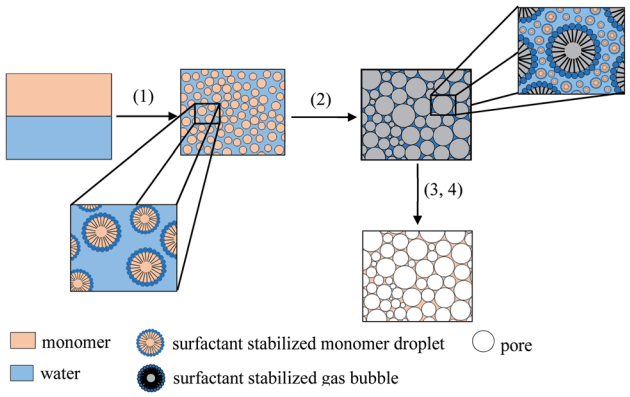

Scheme 1 Concept of the synthesis of polymer foams *via* foamed emulsion templating, redrawn and extended from ref. 30. (1) Preparation of the monomer-in-water emulsion, (2) foaming of the emulsion, (3) polymerization of the monomer within the emulsion, and (4) purification and drying of the polymer foam.

bubble diameter of 46 μm ± 12 μm and highly porous polystyrene foams with a mean pore diameter 76 μm ± 30 μm were obtained.[30] What makes Schüler's study particularly intriguing is a "sub-porosity" in the pore walls caused by the removal of water of the continuous phase after solidification.[30] Porous pore walls may be quite advantageous for some applications such as tissue engineering, because the mobility of substances may be facilitated by the porosity of the pore walls.

To the best of our knowledge, the synthesis of a polymer foam *via* foamed emulsion templating was only carried out with styrene.[30–34] We aim at synthesizing polymer foams *via* foamed emulsion templating by using a biodegradable monomer in order to provide a biocompatible counterpart to the styrene-based polymer foams. The biodegradable PFDMA is assumed to be suitable for this application. However, PFDMA is not purchasable, *i.e.* it has to be synthesized at first. Therefore, we chose the purchasable monomer 1,4-butanediol dimethacrylate (1,4-BDDMA) as scouting system for PFDMA as it was used for the synthesis of polymer foams *via* emulsion templating.[7,8,35] The monomer 1,4-BDDMA is indeed biodegradable[36] but, unfortunately, the polymer is not.[35] The studies in ref. 29 and 30 served as general guidelines for the study at hand. The first goal was to formulate a stable 1,4-BDDMA-in-water emulsion whose foaming led to a stable foamed emulsion. For this purpose, the water-to-glycerol ratio and the monomer content were varied. Having found a suitable emulsion composition, we foamed the 1,4-BDDMA-in-water emulsion by using different stirring speeds and stirring times with the view to adjust the bubble diameters of the foamed emulsion and hence to control the pore diameter of the resulting polymer foam. We successfully synthesized a polymer foam using a foamed emulsion template with a mean pore diameter of 366 μm ± 91 μm. Having synthesized the desired material, we had a closer look at the finestructure of the pore walls and on the mechanism *via* which it is formed.

2. Experimental part

2.1 Materials

1,4-Butanediol dimethacrylate (1,4-BDDMA, 95%) containing 200 ppm to 300 ppm hydroquinone monomethylether (MEHQ), styrene (99%), sodium dodecylsulfate (SDS, ≥99%) and benzoylperoxide (BPO, Luperox® A75, 75%) were purchased from Sigma Aldrich. Glycerol, bi-distilled water (further called water), and ethanol (for Soxhlet extraction) were used. All chemicals were used as received without further purification.

2.2 Formulation, foaming, and polymerization of 1,4-BDDMA-in-water emulsions

The continuous phase of the foamed emulsions was prepared by mixing 1,4-BDDMA, water, glycerol (if applicable) and SDS (calculated with respect to the total mass of the continuous phase of the foamed emulsion), following this order, with a magnetic stirrer for 30 min. The total emulsion volume was 20 ml. Glycerol was added to increase the emulsion's viscosity and thus its stability as reported in Schüler *et al.*[30] In case the polymerization of the foamed emulsion was intended (Section 3.2), 2 mol% of the initiator BPO calculated with respect to the amount (mol) of polymerizable monomer was dissolved in the continuous phase by stirring the emulsion for another 25 min on a magnetic stirrer. Note that no initiator was added to those foamed emulsions whose polymerization was not intended (Section 3.1). The 1,4-BDDMA-in-water emulsion was then treated with a Bandelin SONOPLUS HD-2200 ultrasonic homogenizer for 40 s at a power of ≈30% once (Section 3.1) or three times (Section 3.2) to obtain a homogeneous 1,4-BDDMA-in-water emulsion. For foaming, the emulsion was placed in a vessel and whipped with a KPG stirrer which was equipped with a commercial milk frother. Further below, the mechanical energy used for emulsion foaming is expressed by the stirrer speed. Unless otherwise specified, a stirring speed of 1600 rpm and a stirring time of 4 min was used. Then a microscope image was taken and the foamed emulsion was transferred to a small glass vial (VWR, 44.6 mm × 14.65 mm, $\varnothing_{inner}$ ≈ 1.3 cm) which was filled to a height of ≈3 cm. The free radical polymerization of the foamed emulsion template was induced by UV-light (Heraeus, MH-Modul 250W Z4 XL, à 250 W, spectral range from ≈250 nm to ≈550 nm) for ≈4 h (Section 3.2). In both cases, the two radiation sources were positioned *vis-à-vis* and the foamed emulsion template was placed in between. The poly(1,4-BDDMA) foam was purified *via* Soxhlet extraction with ethanol at 100 °C for a period of at least 12 h and dried at room temperature for at least 48 h.

2.3 Optical microscopy and scanning electron microscopy (SEM)

The monolayers of the foamed emulsion templates were characterized *via* optical microscopy with a Nikon SMZ745T microscope equipped with the high-speed camera Mikroton EoSens CL MC1362. The monolayers were illuminated with an external halogen light source from Schott (KL 1500 Compact) with a power of 150 W connected to a mitos microscope stage from Dolomite *via* an optical fibre. To improve the observability of a monolayer, we followed a procedure described in

literature.[34] Briefly, for the formation of one monolayer, a small amount of the foamed emulsion was confined between two microscope glass slides (76 mm × 52 mm × 1 mm) with a defined distance in between. The distance was set by two strips of an adhesive tape at both ends of the lower microscope glass slide which served as spacers (ESI, Fig. S1†). The thickness of the spacer depended on the used adhesive tapes, which was either ≈52 μm (Sections 3.1.1 and 3.1.2) or ≈55 μm (Sections 3.1.3, 3.1.4 and 3.2) (Tesafilm®, costumer service) because we changed the type of the adhesive tapes once (ESI, Fig. S1†). Afterwards, a microscope picture with a resolution of 1280 × 1024 was taken with the high-speed camera associated software MotionBLITZ® Director2 Kit (Mikroton). By confining the gas bubbles of the foamed emulsion between the two microscope glass slides, the initially spherical bubbles were deformed to cylindrical bubbles. Taking this change of shape into account one can calculate the sizes of the originally spherical bubbles. The bubble diameters of the foamed emulsions were evaluated using the original microscope pictures and the software ImageJ (Section 2.4). For characterizing the poly(1,4-BDDMA) foam *via* scanning electron microscopy (SEM), the polymer foam was cut or broken by using a razor blade. Due to the fragile character of the samples cutting or breaking had to be carried out very carefully. The samples were frozen in liquid nitrogen before treating with a razor blade (cutting or breaking of the sample). An Emitech K550 sputter coater was used to coat the samples with carbon (from Plano), after the samples were fixated on a SEM specimen stub using a silver glue from Plano (Acheson 1415) in order to enhance the sample's conductivity for SEM measurements. The characterization of the poly(1,4-BDDMA) foam in Section 3.2.1, Fig. 4 was carried out with a CamScan CS44 scanning electron microscope (using secondary electron imaging (SEI) and an accelerating voltage of 5 kV). The SEM pictures were taken with the software Edax Genesis at a resolution of 1024 × 800. The pore diameters of the polymer foams were determined from the original SEM pictures taken with the CamScan CS44 SEM and the software ImageJ (Section 2.4). The finestructure of one poly(1,4-BDDMA) foam in Section 3.2.2, Fig. 5, was characterized with a Zeiss GeminiSEM 500 SEM using SEI and an accelerating voltage of 3 kV combined with the user interface SmartSEM from Zeiss. The software ImageJ was further used for improving brightness and contrast of the original SEM pictures and for adding scale bars to the SEM and to the original microscope pictures.

2.4 Determination of bubble and pore diameters

The bubble diameters were calculated by determining the bubble areas within the original two-dimensional microscope pictures (at 5x magnifications (Sections 3.1 and 3.2) or at 4× magnifications (ESI, Fig. S3.1 and S3.2†)) automatically using the software ImageJ. To take the distortion of the spherical bubble shape into account, the volume of the cylindrical bubbles V_{bubble} was calculated by multiplying the area of the bubble A_{bubble} (corresponds to the area of a cylinder) with the thickness of the spacer t_{spacer} (≈52 μm (Sections 3.1.1 and 3.1.2) or ≈55 μm (Sections 3.1.3, 3.1.4 and 3.2) as described in eqn (1)).

$$V_{\text{bubble}} = A_{\text{bubble}} \times t_{\text{spacer}} \quad (1)$$

Knowing the volume of the cylindrical gas bubble, which is the same volume as that of the spherical gas bubble V_{bubble}, the bubble diameter d_{bubble} of the originally spherical bubble can be calculated by using eqn (2).

$$d_{\text{bubble}} = 2 \times \left(\frac{3 \times V_{\text{bubble}}}{4 \times \pi}\right)^{\frac{1}{3}} \quad (2)$$

A total number n_{total} of 100 gas bubbles was considered followed by the calculation of the arithmetic mean $\bar{d}_{\text{bubble}}$ and its standard deviation σ (eqn (4) and (5)).

For the determination of the pore diameters of the polymer foam, the area of each pore A_{pore} was determined by encircling the pores manually within the original two-dimensional SEM pictures (at 20× magnifications) made with the CamScan CS44 SEM (1) using ImageJ. Each pore was treated as a sphere and the pore diameter d_{pore} was calculated by using eqn (3). A total number of 100 pores was considered followed by the calculation of the arithmetic mean $\bar{d}_{\text{pore}}$ and its standard deviation σ using eqn (4) and (5).

$$d_{\text{pore}} = 2 \times \sqrt{\frac{A_{\text{pore}}}{\pi}} \quad (3)$$

$$\bar{d}_{\text{bubble/pore}} = \frac{1}{n_{\text{total}}} \times \sum_{i=1}^{n_{\text{total}}} d_{\text{bubble},i/\text{pore},i} \quad (4)$$

$$\sigma = \sqrt{\frac{\sum_{i=1}^{n_{\text{total}}} \left(d_{\text{bubble},i/\text{pore},i} - \bar{d}_{\text{bubble/pore}}\right)^2}{n_{\text{total}} - 1}} \quad (5)$$

The distribution of the bubble and pore diameters were graphically illustrated with the software SigmaPlot by plotting the fraction of number of bubbles or pores n over n_{total} (=100) within a certain diameter range *versus* the diameter d. The polydispersity index (PDI) of the foamed emulsion templates and of the polymer foam was calculated by using eqn (6).

$$\text{PDI} = \frac{\sigma}{\bar{d}_{\text{bubble/pore}}} \times 100 \quad (6)$$

For the readers' information, the quantitative characterization of all foamed emulsions and the polymer foam (d_{bubble}, $\bar{d}_{\text{bubble}} \pm \sigma$, PDI, d_{pore}, $\bar{d}_{\text{pore}} \pm \sigma$, PDI) is based only on the approach mentioned in this Section. Thus, the mathematically calculated mean diameters differ slightly from the estimated mean diameters that can be extracted from the bubble and pore size distributions (Section 3.2, Fig. 4). The mathematically calculated standard deviation of the mean diameter is probably lower than the "real error" (including systematical and randomly made errors).

2.5 Interfacial tension measurements

Interfacial tensions were measured using the pendant drop profile analysis tensiometer PAT-1 from Sinterface. At first, a drop of 1,4-BDDMA or styrene was either generated in the aqueous phase or in the aqueous phase containing 20 vol% glycerol, respectively. The interfacial tensions were measured after 1800 s (30 min).

3. Results and discussions

3.1 Formulation and foaming of 1,4-BDDMA-in-water emulsions

3.1.1 1,4-BDDMA-in-water emulsions *vs.* styrene-in-water emulsions. An emulsion composition that met the following requirements was searched for: the emulsion had to be foamable and stable before, during and after foaming as well as during polymerization. The study of Schüler *et al.* served as general guideline where the continuous phase consisted of 65 vol% styrene, 20 vol% water, 15 vol% glycerol, stabilized by 5 wt% SDS.[30] The mass of the surfactant SDS was calculated related to the total mass of the emulsion. Using this composition as starting point, we generated a foamed 1,4-BDDMA-in-water emulsion and monitored its stability. For this purpose, monolayers of the foamed emulsion were analyzed directly after foaming, $\approx$2 h after foaming, and $\approx$4 h after foaming using optical microscopy. For the sake of comparison, a foamed styrene-in-water emulsion of the same composition were also generated and characterized. In both cases, foaming was carried out by using a stirring speed of 1600 rpm for a stirring time of 4 min, which was found to be the best setting in ref. 30. The micrographs of the foamed emulsion monolayers are shown in Fig. 1.

Looking at the microscope pictures of the 1,4-BDDMA-containing emulsion (Fig. 1, left), one observes that (a) the gas bubble sizes increase and (b) the emulsion decomposes over time. The latter is revealed by the brightening of the continuous phase from deeply black to washy grey. As for the styrene-containing foamed emulsion, the gas bubbles also increase over time but the emulsion did not decompose (Fig. 1, right). The first observation, *i.e.* the increase of the gas bubbles, is caused by the floating-up of gas bubbles from the lower part of the foamed emulsion as well as by Ostwald ripening or coalescence at longer times which is in line with the time evolution of the mean bubble diameters (ESI, Fig. S2.1†). To sum up, the bubbles of the foamed emulsions increase over time for both systems. However, only the 1,4-BDDMA-in-water emulsion decomposes over time. Thus, an emulsion composition of 65 vol% monomer, 20 vol% water, 15 vol% glycerol, stabilized by 5 wt% SDS (calculated with respect to the total mass of the continuous phase) works for styrene-containing emulsions and foamed emulsions but is obviously not directly transferable to other monomer-in-water emulsions. We suspected glycerol to have a negative impact on the emulsion stability although it increases the viscosity of the continuous phase and should thus have a stabilizing effect.[30] To find an explanation for the low emulsion stability, we carried out interfacial tension measurements. The interfacial tension between the monomer and water as well as between the monomer and an aqueous solution containing 20 wt% glycerol was measured. The interfacial tension between 1,4-BDDMA and water was 14.4 mN m^{-1} and decreased dramatically to 7.2 mN m^{-1} by adding glycerol, while the interfacial tension between styrene and water was 27.2 mN m^{-1} and remained nearly unchanged with a value of 26.7 mN m^{-1} upon addition of glycerol to the aqueous phase. These measurements reveal that the interfacial tension between styrene and water is nearly twice as high as the one between 1,4-BBDMA and water. Moreover, the impact of glycerol on the interfacial tension is much stronger in case of 1,4-BDDMA. Why has glycerol such a huge impact on the interfacial tension and therefore on the stability of the 1,4-BDDMA-in-water emulsion? An explanation can be given looking at the molecular structures of the chemicals used (ESI, Fig. S2.2†). Comparing the molecular structures of both monomers, one sees that 1,4-BDDMA is more hydrophilic than styrene due to its two ester groups which was confirmed by our interfacial tension measurements. We assume that the higher hydrophilicity and the presence of two ester groups enable strong interactions between 1,4-BDDMA and glycerol *via* hydrogen bonding, as glycerol carries three hydroxyl groups. Thus, it is conceivable that, beside the surfactant molecules, glycerol molecules of the aqueous phase are also captured at the 1,4-BDDMA/water interface. As a result, the SDS molecules cannot form a tightly packed surfactant layer at the interface between 1,4-BDDMA and water, which, in turn, facilitates emulsion disintegration mechanisms such as coalescence. Styrene, on the other hand, provides no polar groups or H-bond acceptor groups whatsoever. Thus, interactions between the glycerol in the aqueous phase and styrene are unlikely. Consequently, SDS molecules can form tightly packed surfactant layers at the interface between styrene and water. Furthermore, the higher interfacial tension between styrene and water provides a stronger driving force for surfactant adsorption at the oil/water interface. To sum up, we considered glycerol to act as disturbing "co-surfactant" at the interface between the monomer 1,4-BDDMA and water. Since glycerol still contributes favorably to the stabilization of the foamed emulsion by increasing the viscosity of the continuous phase we had to find an optimal ratio between 1,4-BDDMA, water, and glycerol.

3.1.2 Variation of the water-to-glycerol ratio. As mentioned in Schüler *et al.*, 64 vol% is the highest volume of spherical monomer droplets which is dispersible in a densely packed, disordered, polydisperse monomer-in-water emulsion without jamming and distortion of the monomer droplets.[30] Therefore, we kept the volume of 1,4-BDDMA in the 1,4-BDDMA-in-water emulsion constant at 65 vol% and varied the water-to-glycerol ratio to find the optimum composition of the continuous phase of the foamed emulsion. The surfactant concentration was 5 wt% of the total emulsion mass as in ref. 30. The volume of water was successively decreased from 35 vol% to 20 vol%, while the volume of glycerol was increased from 0 vol% to 15 vol% (Table 1). Foaming was carried out using a stirring speed of 1600 rpm for a stirring time of 4 min. The stability of the emulsion was determined by monitoring the microscope pictures of the monolayers of the foamed emulsions. The stability of the corresponding foamed emulsion was monitored by observing the height of a column of the foamed emulsion over a period of 24 h (not shown here). Fig. 2 shows the

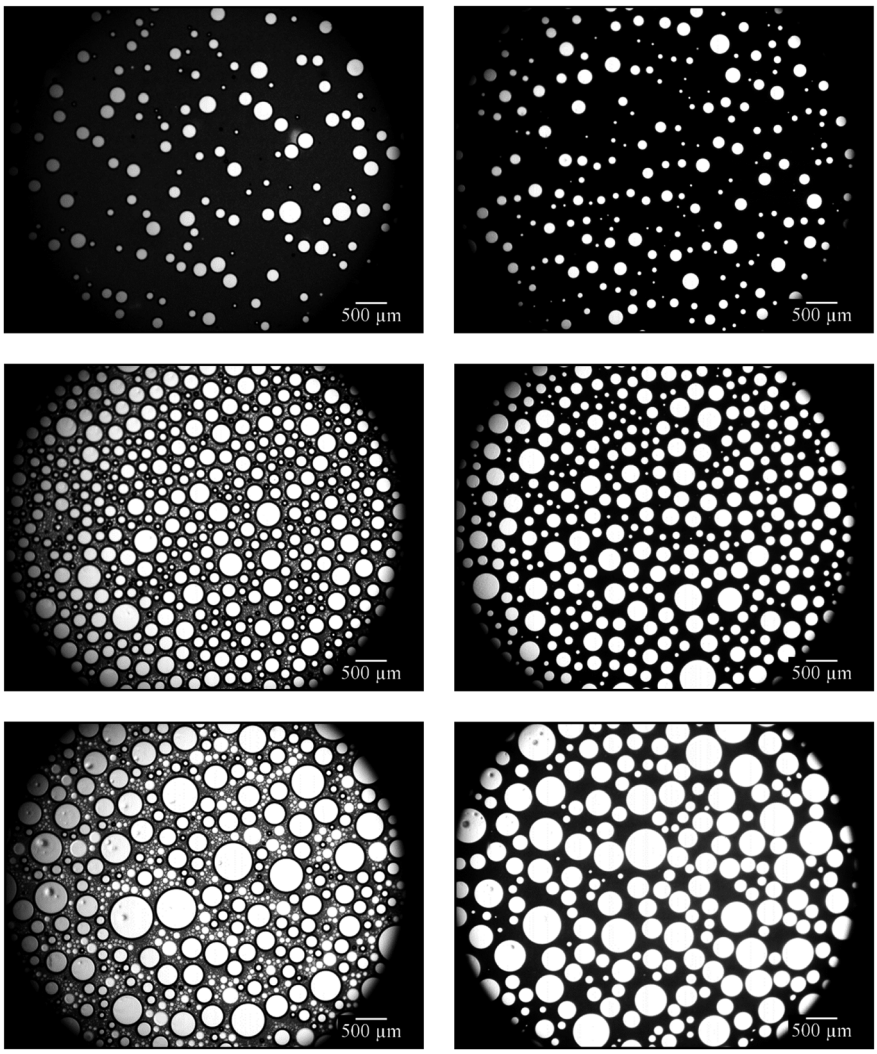

Fig. 1 Microscope pictures of monolayers of foamed 1,4-BDDMA-in-water emulsions (left) and of foamed styrene-in-water emulsions (right) taken directly after foaming (top), after ≈2 h (middle), and after ≈4 h (bottom). The continuous phase of the foamed emulsions consisted of 65 vol% monomer, 20 vol% water, 15 vol% glycerol and was stabilized by 5 wt% SDS (calculated with respect to the total mass of the continuous phase). The dispersed phase was air. The foamed emulsions were generated *via* a stirring speed of 1600 rpm for a stirring time of 4 min. All microscope pictures were made with 5× magnification.

Table 1 Volume fractions of water and glycerol in the continuous phase of the foamed emulsion. The residual continuous phase contained 65 vol% 1,4-BDDMA and is stabilized by 5 wt% SDS (calculated with respect to the total mass of the continuous phase). The dispersed phase was air

Sample number	1,4-BDDMA/vol%	Water/vol%	Glycerol/vol%
(1)	65	35	0
(2)	65	30	5
(3)	65	25	10
(4)	65	20	15

monolayers with increasing glycerol content in the 1,4-BDDMA-in-water emulsions.

Fig. 2 shows that the continuous phase between the gas bubbles becomes increasingly grey and translucent with increasing glycerol content. As already mentioned in Section 3.1.1, this is a sign for emulsion disintegration. This observation confirms our assumption that glycerol acts as a disturbing "co-surfactant" if the glycerol content in the aqueous phase of the emulsion is too high. However, the foamability and the stability of the foamed emulsions increased with increasing glycerol concentration (data not shown). In conclusion, glycerol noticeably destabilizes the 1,4-BDDMA-in-water emulsions at concentrations > 5 vol% but stabilizes at the same time the foamed emulsions. The stabilizing effect on the foamed emulsion can be ascribed to the high viscosity of glycerol which slows down foam drainage.[30] As a compromise, a glycerol concentration of 5 vol% was chosen for further emulsion compositions. Looking at the mean bubble diameters (ESI, Fig. S2.3†) of the four monolayers in Fig. 2, one sees no significant change of the bubble size although the viscosity of the continuous phase was different.

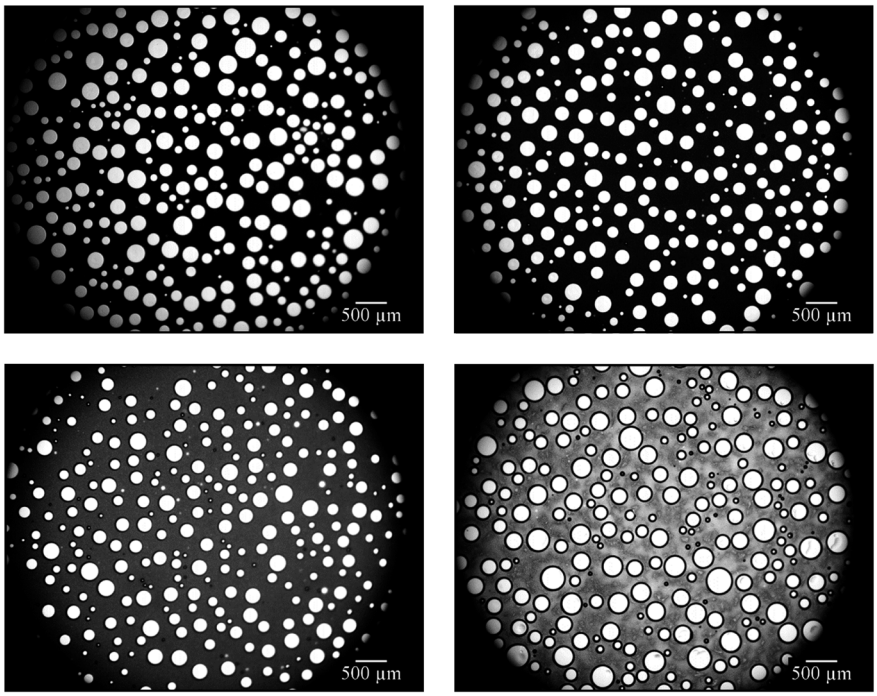

Fig. 2 Microscope pictures of monolayers of foamed 1,4-BDDMA-in-water emulsions with different water-to-glycerol volume ratios, namely 35 : 0 (top left), 30 : 5 (top right), 25 : 10 (bottom left), and 20 : 15 (bottom right) taken directly after foaming. The residual continuous phase of the emulsion contained 65 vol% 1,4-BDDMA and was stabilized by 5 wt% SDS (calculated with respect to the total mass of the continuous phase). The dispersed phase was air. All emulsions were foamed by using a stirring speed of 1600 rpm for a stirring time of 4 min. All microscope pictures were made with 5× magnification.

3.1.3 Variation of the 1,4-BDDMA content. Schüler *et al.* kept the amount of styrene constant at 65 vol% to prevent or minimize the jamming of the styrene droplets.[30] Therefore, we started with the same content of monomer. The experiments described in this study indicate 65 vol% 1,4-BDDMA, 30 vol% water and 5 vol% glycerol to be a promising emulsion composition to formulate a stable 1,4-BDDMA-in-water emulsion and a stable foamed emulsion over time as well. This is confirmed by the emulsion stability and the foam stability measured over a period of ≈4 h shown on the left-hand side of Fig. 3. The microscope pictures tell the same story as those of the styrene-based foamed emulsions shown in Fig. 1 (right): the emulsion remains stable, while the gas bubbles increase over time (ESI, Fig. S2.4†).

On the other hand, Salonen *et al.* were able to foam an oil-in-water emulsion with a dispersed phase volume of 70 vol% using an unpolymerizable oil in which the jamming of oil droplets slowed down drainage and thus increased the stability of the foamed emulsion.[29] In order to generate an emulsion with a monomer content as high as possible, we used a monomer content of 75 vol% and reduced the water content to 20 vol%. The surfactant concentration was kept constant at 5 wt% (calculated with respect to the total mass of the continuous phase). Foaming was carried out by using a stirring speed of 1600 rpm for a stirring time of 4 min. The stability of the continuous phase of the foamed emulsion, *i.e.* the 1,4-BDDMA-in-water emulsion, was studied *via* optical microscopy of the respective foamed emulsion monolayers over a period of ≈4 h. The right-hand side of Fig. 3 shows the monolayer of the foamed 1,4-BDDMA-in-water emulsions consisting of 75 vol% 1,4-BDDMA, 20 vol% water, and 5 vol% glycerol.

The microscope picture in Fig. 3 (top right) shows the monolayer of a foamed 1,4-BDDMA-in-water emulsion containing 75 vol% monomer directly after foaming. Comparing this microscope picture with those taken after a 2 h and 4 h, respectively (Fig. 3, middle right, bottom right), one sees that most of the bubbles disappeared, while the mean bubble size increased (ESI, Fig. S2.4†) caused by destabilization effects as explained in Section 3.1.1. If one compares the microscope pictures of foamed emulsions containing 65 vol% 1,4-BDDMA (Fig. 3, left) with those containing 75 vol% 1,4-BDDMA (Fig. 3, right), it becomes obvious that the foaming behavior is much better for the former foamed emulsion. Additionally, the mean bubble diameters of the foamed emulsions containing 65 vol% 1,4-BDDMA are larger compared to those obtained with 75 vol% monomer (ESI, Fig. S2.4†). The reason for this finding is not understood yet.

At a monomer content of 75 vol%, the so-called "jamming-regime" is reached,[37] *i.e.* the monomer droplets are tightly-packed and start to deform (the monomer droplets are no longer spherical). Due to this packaging, monomer droplets are jammed into the liquid films between neighboring bubbles. As the anionic surfactant SDS was used to stabilize the monomer droplets of the emulsion and the bubbles of the foamed emulsion, all monomer droplets and bubbles are negatively charged, which leads to two effects. (1) The positive effect is electrostatic

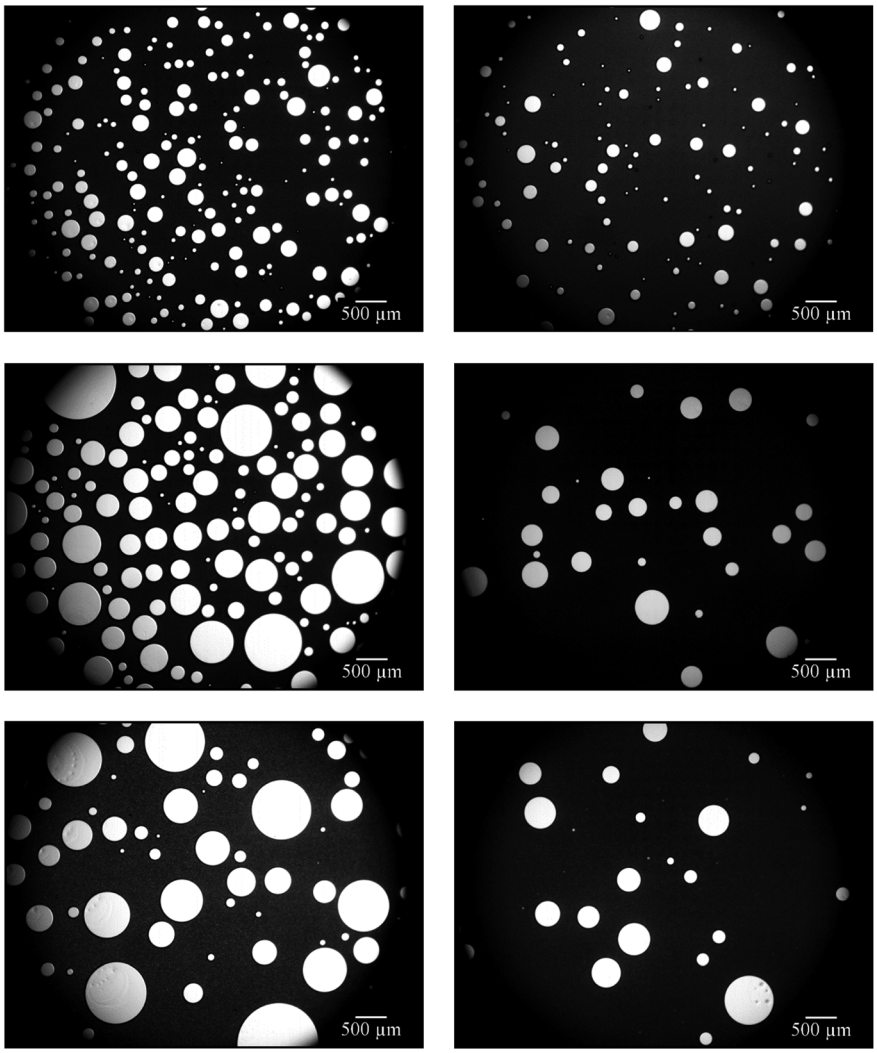

Fig. 3 Microscope pictures of monolayers of foamed 1,4-BDDMA-in-water emulsions consisting of 65 vol% 1,4-BDDMA, 30 vol% water, and 5 vol% glycerol (left) and 75 vol% 1,4-BDDMA, 20 vol% water, and 5 vol% glycerol (right). The foamed emulsions were stabilized by 5 wt% SDS (calculated with respect to the total mass of the continuous phase) (right). The dispersed phase was air. The emulsions were foamed by using a stirring speed of 1600 rpm for a stirring time of 4 min. The microscope pictures were taken directly after foaming (top), after ≈2 h (middle), and after ≈4 h (bottom). All microscope pictures were made with 5× magnification.

droplet/bubble repulsion leading to a fixation of the monomer droplets within the liquid films and thus slowing down drainage. (2) The negative effect is electrostatic droplet/droplet repulsion. Adjacent monomer droplets trapped within the liquid films between the bubbles repel each other leading to a repulsive pressure at the water/air interfaces. Since there are much more emulsion droplets than bubbles in the foamed emulsion, the droplet/droplet repulsion dominates and thus the stability of the foamed emulsion is reduced (bubbles burst due to the pressure). To conclude, the negative surface charge of the monomer droplets destroys the foam once the "jamming regime" (>64 vol%) is surpassed. However, below the jamming regime (≤64 vol%), the presence of monomer droplets within the Plateau borders could be conducive by slowing-down drainage.[30]

3.1.4 Variation of foam generation settings. After having found the optimum composition of the continuous phase of the foamed 1,4-BDDMA-in-water emulsion (65 vol% 1,4-BDDMA, 30 vol% water, 5 vol% glycerol) we were interested in generating polydisperse foamed emulsions of different bubble sizes. As described by Schüler *et al.*, we wanted to study the relation between the stirring speed, the stirring time and the resulting bubble and pore sizes with the aim to control the latter.[30] The 1,4-BDDMA-in-water emulsions were prepared and foamed as described in Section 2.2. According to Schüler *et al.*, stirring speeds of 1600 rpm, 1200 rpm, 900 rpm, or 600 rpm were used and at each stirring speed stirring times of 2 min, 4 min or 8 min were set.[30]

We found that the mechanical energy induced by stirrer speeds of 1600 rpm and 1200 rpm leads to no significant change of the bubble sizes (Table 2, the monolayers are shown in the ESI (Fig. S3.1 and S3.2†)). Thus, stirring speeds of 900 rpm and 600 rpm were not tested. Furthermore, the stirring time also had no impact on the bubble size as can be seen in Table 2. This

Table 2 Stirring speeds and stirring times for the generation of foamed emulsion templates. Mean bubble diameters $\bar{d}_{bubble}$ and PDIs of the monolayers of foamed emulsion templates consisting of 65 vol% 1,4-BDDMA, 30 vol%, 5 vol% glycerol. The continuous phase contained 5 wt% SDS (calculated with respect to the total mass of the continuous phase) and 2 mol% BPO (calculated with respect to the total amount (mol) of the monomer 1,4-BDDMA). For the calculation of the mean bubble diameters 100 bubbles were considered (n_{total} = 100)

Foam generation settings		Foamed emulsion template	
Stirring speed/rpm	Stirring time/min	$\bar{d}_{bubble}$/μm	PDI/%
1600	2	137 ± 80	59
1600	4	151 ± 90	59
1600	8	124 ± 59	47
1200	4	167 ± 92	55
1200	8	145 ± 80	55

outcome was unexpected as Schüler *et al.* generated styrene-based foamed emulsions with different bubble diameters between ≈160 μm and ≈40 μm by changing the stirring speeds and the stirring times.[30] So far, we have no explanation for this finding. We will not further investigate the influence of the stirring parameters since this is beyond the scope of our study. The primary aim of the study at hand was to find an optimum composition of the 1,4-BDDMA-in-water emulsion and the foamed emulsion thereof to check their suitability as templates for the synthesis of polymer foams. Thus, the foamed emulsion generated *via* a stirring speed of 1600 rpm and a stirring time of 4 min (compare Fig. 2, top right, Fig. 3, top left) was polymerized.

3.2 Solid polymer foam *via* foamed emulsion templating

3.2.1 Polymerization of foamed 1,4-BDDMA-in-water emulsions. Our study is pursued by polymerizing one foamed emulsion template. The continuous phase of the foamed emulsion consisted of 65 vol% 1,4-BDDMA, 30 vol% water, and 5 vol% glycerol. The continuous phase further contained 5 wt% SDS calculated with respect to the total mass of the continuous phase. For initiation of the monomer, 2 mol% BPO with respect to the amount (mol) of the monomer 1,4-BDDMA was used. The foamed emulsions were generated using a stirring speed of 1600 rpm and a stirring time of 4 min. Comparable microscope pictures of the foamed emulsion are shown in Fig. 2 (top right) and Fig. 3 (top left), while a SEM picture of the polymerized foamed emulsion is shown in Fig. 4 (left). Note that the mean bubble diameters of the foamed emulsion used in this section for polymerization and of the foamed emulsion shown in Fig. 2 (top right) and Fig. 3 (top left) slightly differ (compare with ESI, Fig. S.2.3 and S.2.4†).

The left hand side of Fig. 4 shows the resulting SEM micrograph, while the bubble size distribution of the foamed emulsion monolayer as well as the pore size distribution of the polymer foam is shown on the right. Comparing the mean pore diameter of the solid polymer foam, 366 μm ± 91 μm (PDI = 25%), in Fig. 4 with the mean bubble diameters of the foamed emulsions, 151 μm ± 90 μm (PDI = 59%), in Fig. 2 (top right) and Fig. 3 (top left) one sees that the pores are about twice as large as the bubbles. The reasons for the increase of the pore diameter with respect to the bubble diameter are Ostwald ripening and coalescence which occur in the foamed emulsion template until a certain degree of solidification is reached (compare with Section 3.1).

3.2.2 Finestructure of the resulting polymer foam. So far, we were able to synthesize a poly(1,4-BDDMA) foam *via* polymerization of a foamed 1,4-BDDMA-in-water emulsion. But why does the polymerization of disordered monomer droplets dispersed in an aqueous phase lead to a polymer foam structure rather than to individual polymer particles? A possible explanation was given by Elsing *et al.* who studied the synthesis of polystyrene foams *via* polymerization of foamed styrene-in-

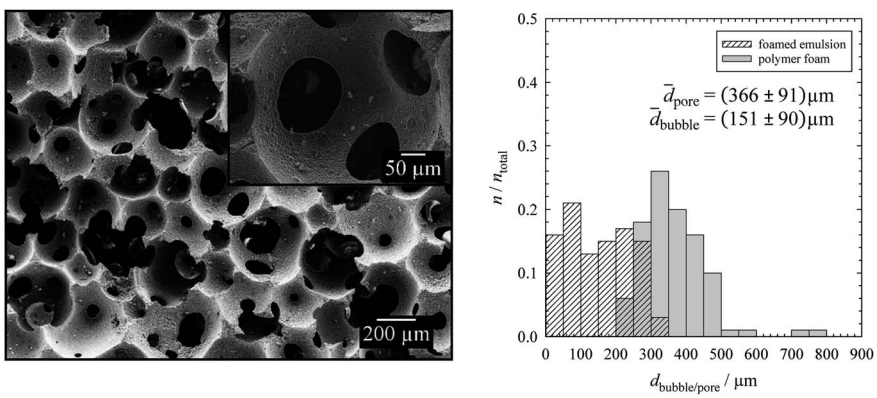

Fig. 4 SEM pictures of a specimen of a poly(1,4-BDDMA) foam synthesized from a foamed 1,4-BDDMA-in-water emulsion consisting of 65 vol% 1,4-BDDMA, 30 vol% water, and 5 vol% glycerol. The continuous phase contained 5 wt% SDS (calculated with respect to the total mass of the continuous phase) and 2 mol% BPO (calculated with respect to the amount (mol) of the monomer 1,4-BDDMA). The dispersed phase was air. The emulsion was foamed by using a stirring speed of 1600 rpm for a stirring time of 4 min. The bubble size distribution of the foamed emulsion template and the corresponding pore size distribution of the polymer foam each with n_{total} = 100 are shown on the right. The SEM pictures were made with 50× and 250× magnifications.

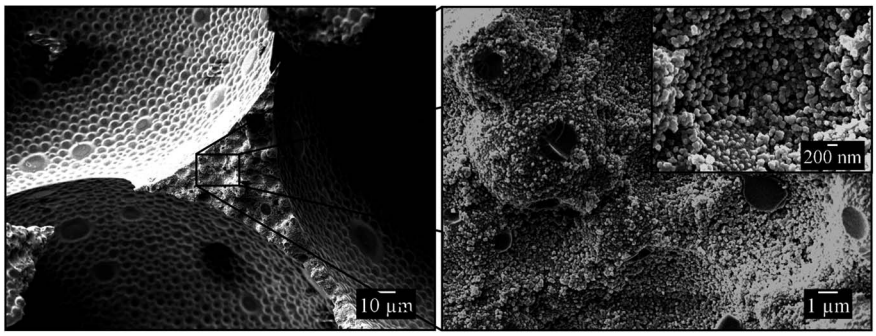

Fig. 5 SEM picture of a fracture of a poly(1,4-BDDMA) foam at the vertex (left). Close-up SEM pictures of zooms in the finestructure of the highlighted area in the left SEM picture (right). The poly(1,4-BDDMA) foam was synthesized from a foamed 1,4-BDDMA-in-water emulsion consisting of 65 vol% 1,4-BDDMA, 30 vol% water, and 5 vol% glycerol. The emulsion contained 5 wt% SDS (calculated with respect to the total mass of the continuous phase) and 2 mol% BPO (calculated with respect to the amount (mol) of the monomer 1,4-BDDMA). The dispersed phase was air. The SEM pictures were made with 500×, 5000×, and 25 000× magnifications.

water emulsions.[32,34] It was suggested that the formation of the polymer foam matrix is a result of polystyrene chains between the monomer droplets which are formed during the polymerization. These chains link the monomer droplets and hence connect them during polymerization. To get to the bottom of this, we had a closer look at the finestructure of our poly(1,4-BDDMA) foam using a scanning electron microscope with a higher resolution. We examined a fracture of a polymer foam which was prepared from a foamed emulsion consisting of 65 vol% 1,4-BDDMA, 30 vol% water, and 5 vol% glycerol. The monomer-in-water emulsion contained 5 wt% SDS (with respect to the total mass of the continuous phase) and 2 mol% BPO (calculated with respect to the amount (mol) of monomer 1,4-BDDMA). The results can be seen in Fig. 5.

Fig. 5 shows three SEM pictures of the same fractured vertex of the 1,4-BDDMA-based polymer foam (the area between 3 pores in a two-dimensional SEM picture) with increasing magnifications. The SEM picture on the left of Fig. 5 suggests a rough and uneven surface of the vertex cross-section which is confirmed by zooming into the finestructure (Fig. 5, right). The close-up SEM pictures, reveal that the continuous phase of the polymer foam consists of densely-packed polymer globules of different sizes with voids in between. The polymer globules originate from the polymerization of monomer droplets which were dispersed in the aqueous phase to form the monomer-in-water emulsion and build up the polymer foam's continuous phase. The voids between the interconnected globules, in turn, originate from the evaporation of the surrounding aqueous phase after solidification of the foamed emulsion and creates a "sub-porosity" within the pore walls. This structure is very similar to that found in polystyrene foams prepared from foamed styrene-in-water emulsions by Elsing *et al.*[32,34] For these polystyrene foams it could be shown that the porosity of the polymer foam's continuous phase matches exactly the aqueous phase volume fraction of the foamed emulsion template. This should also be the case for the polymer foam seen in Fig. 5. In general, the porosity of poly(1,4-BDDMA) foams will be measured and discussed in a follow-up study. In summary, the synthesized poly-1,4-BDDMA foam exhibits a two-fold porosity: the main porosity of the polymer foam is given by the bubbles of the template, while the "sub-porosity" is given by the amount of water in the continuous phase of the template.

4. Conclusion and outlook

The first part of the paper at hand deals with the formulation and foaming of 1,4-BDDMA-in-water emulsions and the possibility to obtain a polymer foam *via* polymerization of the foamed emulsion. The idea was to use foamed 1,4-BDDMA-in-water emulsions as structure-giving templates to yield a polymer foam with large pore diameters and porous pore walls as already shown for polystyrene foams.[31–34] To achieve this, we first looked for an optimum composition of the emulsion, *i.e.* the continuous phase of the foamed emulsion. The emulsion had to meet the following requirements: the monomer-in-water emulsion had to be foamable and stable against emulsion disintegration before, during, and after foaming and during polymerization. For this purpose, we varied each component of the monomer-in-water emulsion systematically and finally ended up with an optimum emulsion composition consisting of 65 vol% 1,4-BDDMA, 30 vol% water, and 5 vol% glycerol. SDS (5 wt%) was used to stabilize both the emulsion and the foamed emulsion. We explain in detail why the composition is crucial for the formulation and the stability of the foamed emulsion.

The second part of this study focusses on the synthesis of a poly(1,4-BDDMA) foam *via* polymerization of a foamed 1,4-BDDMA-in-water emulsion template. We were able to polymerize a foamed emulsion with a mean bubble diameter of 151 µm ± 90 µm and obtained a highly porous poly(1,4-BDDMA) foam with a mean pore diameter of 366 µm ± 91 µm. A closer look at the finestructure of the poly(1,4-BDDMA) foam revealed that the polymer foam's continuous phase is also porous. The "sub-porosity" of the polymer foam's continuous phase comes from the aqueous phase of the 1,4-BDDMA-in-water emulsion. The latter will be demonstrated in a follow-up study. After having found an optimum composition for formulating, foaming, and polymerizing 1,4-BDDMA-in-water emulsions, our future work will deal with the synthesis of monodisperse poly(1,4-BDDMA) foams as counterpart to the studies about monodisperse polystyrene foams prepared from foamed styrene-in-water

emulsions.[31–34] Moreover, after having finished our investigations with the scouting system 1,4-BDDMA, we will synthesize biodegradable, monodisperse PFDMA-based polymer foams with defined morphologies. Ultimately, the aim is to test the suitability of PFDMA-based polymer foams for tissue engineering applications.

Conflicts of interest

The authors declare no conflicts of interests.

Acknowledgements

The authors would like to thank E. Öztürk for her preliminary work on the emulsion composition during her internship and S. Varitimiadou for the generation of the foamed 1,4-BDDMA-in-water emulsions in Section 3.1.4 (including ESI, S3.1 and S3.2†) and for the generation and polymerization of the foamed emulsion template in Section 3.2 during her internship. We are thankful to A. Fels for his help with the CamScan CS44 SEM and Y. Qawasmi for taking the two SEM pictures at high magnifications with the Zeiss GeminiSEM 500 SEM. Finally, we thank A. Salonen, W. Drenckhan, and J. Elsing for helpful discussions.

References

1 C. Stubenrauch, A. Menner, A. Bismarck and W. Drenckhan, *Angew. Chem., Int. Ed.*, 2018, **57**, 10024.
2 S. Yang, K.-F. Leong, Z. Du and C.-K. Chua, *Tissue Eng.*, 2001, **7**, 679.
3 P. X. Ma, *Mater. Today*, 2004, **7**, 30.
4 F. J. O'Brien, *Mater. Today*, 2011, **14**, 88.
5 P. A. De Bank, M. D. Jones and M. J. Ellis, Polymeric Scaffolds for Regenerative Medicine, in *Macroporous Polymers. Production Properties and Biotechnological/Biomedical Applications*, ed. B. Mattiasson, A. Kumar and I. Y. Galaev, CRC Press (Taylor and Francis Group), Boca Raton, 2010, ch 16, pp. 467–495.
6 E. M. Christenson, W. Soofi, J. L. Holm, N. R. Cameron and A. G. Mikos, *Biomacromolecules*, 2007, **8**, 3806.
7 J. L. Robinson, R. S. Moglia, M. C. Stuebben, M. A. P. McEnery and E. Cosgriff-Hernandez, *Tissue Eng., Part A*, 2014, **20**, 1103.
8 R. S. Moglia, M. Whitely, P. Dhavalikar, J. Robinson, H. Pearce, M. Brooks, M. Stuebben, N. Cordner and E. Cosgriff-Hernandez, *Biomacromolecules*, 2014, **15**, 2870.
9 A. Barbetta, E. Barigelli and M. Dentini, *Biomacromolecules*, 2009, **10**, 2328.
10 A. Barbetta, M. Dentini, M. S. De Vecchis, P. Filippini, G. Formisano and S. Caiazza, *Adv. Funct. Mater.*, 2005, **15**, 118.
11 A. Barbetta, M. Dentini, E. M. Zannoni and M. E. De Stefano, *Langmuir*, 2005, **21**, 12333.
12 A. Barbetta, M. Massimi, B. Di Rosario, S. Nardecchia, M. De Colli, L. Conti Devirgiliis and M. Dentini, *Biomacromolecules*, 2008, **9**, 2844.
13 J. Miras, S. Vílchez, C. Solans and J. Esquena, *J. Colloid Interface Sci.*, 2013, **410**, 33.
14 J. Miras, S. Vílchez, C. Solans, T. Tadros and J. Esquena, *Soft Matter*, 2013, **9**, 8678.
15 S. Vílchez, L. A. Pérez-Carrillo, J. Miras, C. Solans and J. Esquena, *Langmuir*, 2012, **28**, 7614.
16 M. Costantini, C. Colosi, J. Guzowski, A. Barbetta, J. Jaroszewicz, W. Święszkowski, M. Dentini and P. Garstecki, *J. Mater. Chem. B*, 2014, **2**, 2290.
17 A. Testouri, C. Honorez, A. Barillec, D. Langevin and W. Drenckhan, *Macromolecules*, 2010, **43**, 6166.
18 A. Barbetta, A. Carrino, M. Costantini and M. Dentini, *Soft Matter*, 2010, **6**, 5213.
19 S. Andrieux, W. Drenckhan and C. Stubenrauch, *Polymer*, 2017, **126**, 425.
20 S. Andrieux, W. Drenckhan and C. Stubenrauch, *Langmuir*, 2018, **34**, 1581.
21 S. Andrieux, A. Quell, C. Stubenrauch and W. Drenckhan, *Adv. Colloid Interface Sci.*, 2018, **256**, 276.
22 S. Andrieux, L. Medina, M. Herbst, L. A. Berglund and C. Stubenrauch, *Composites, Part A*, 2019, **125**, 105516.
23 A. Barbetta, A. Gumiero, R. Pecci, R. Bedini and M. Dentini, *Biomacromolecules*, 2009, **10**, 3188.
24 J.-y. Lin, W.-j. Lin, W.-h. Hong, W.-c. Hung, S. H. Nowotarski, S. Montenegro Gouveia, I. Cristo and K.-h. Lin, *Soft Matter*, 2011, **7**, 10010.
25 C. Claaßen, M. H. Claaßen, V. Truffault, L. Sewald, G. E. M. Tovar, K. Borchers and A. Southan, *Biomacromolecules*, 2018, **19**, 42.
26 C. Claaßen, A. Southan, J. Grübel, G. E. M. Tovar and K. Borchers, *Biomed. Mater.*, 2019, **13**, 055008.
27 L. Sewald, C. Claaßen, T. Götz, M. H. Claaßen, V. Truffault, G. E. M. Tovar, A. Southan and K. Borchers, *Macromol. Biosci.*, 2018, **18**, 1800168.
28 F. Dehli, L. Rebers, C. Stubenrauch and A. Southan, *Biomacromolecules*, 2019, **20**, 2666.
29 A. Salonen, R. Lhermerout, E. Rio, D. Langevin and A. Saint-Jalmes, *Soft Matter*, 2012, **8**, 699.
30 F. Schüler, D. Schamel, A. Salonen, W. Drenckhan, M. D. Gilchrist and C. Stubenrauch, *Angew. Chem., Int. Ed.*, 2012, **51**, 2213.
31 A. Quell, J. Elsing, W. Drenckhan and C. Stubenrauch, *Adv. Eng. Mater.*, 2015, **17**, 604.
32 J. Elsing, T. Stefanov, M. D. Gilchrist and C. Stubenrauch, *Phys. Chem. Chem. Phys.*, 2017, **19**, 5477.
33 J. Elsing, A. Quell and C. Stubenrauch, *Adv. Eng. Mater.*, 2017, 1700195.
34 J. Elsing, Foamed Styrene-in-Water Emulsions as Template for Highly Ordered Polystyrene Foams, PhD thesis, Universität Stuttgart, Shaker-Verlag, Aachen, 2017, ISBN 978-3-8440-5264-0.
35 M. L. Dabrowski, D. Jenkins, E. Cosgriff-Hernandez and C. Stubenrauch, *Phys. Chem. Chem. Phys.*, 2020, **22**, 155.
36 S. Cousinet, A. Ghadban, E. Fleury, F. Lortie, J.-P. Pascault and D. Portinha, *Eur. Polym. J.*, 2015, **67**, 539.
37 W. Drenckhan and D. Langevin, *Curr. Opin. Colloid Interface Sci.*, 2010, **15**, 341.

